arXiv:1601.02755v1 [cond-mat.stat-mech] 12 Jan 2016

U(1) Emergence versus Chiral Symmetry Restoration in the Ashkin Teller Model

Soumyadeep Bhattacharya*
Institute of Mathematical Sciences, CIT Campus, Taramani, Chennai 600113, India
(Dated: January 13, 2016)

We show that suppression of vortices in the Ashkin Teller ferromagnet on a square lattice splits the order-disorder transition and opens up an intermediate phase where the macroscopic symmetry enhances to U(1). When we selectively suppress the formation of non-chiral vortices, chiral vortices proliferate and replace the U(1) phase with a new phase where chiral symmetry is restored. This result demonstrates a fascinating phenomenon in which the symmetry information encoded in topological defects manifests itself in the symmetry of the phase where the defects proliferate. We also show that this phenomenon can occur in all $\mathbb{Z}_n$ ferromagnets with even values of n.

Topological defects play a crucial role in enhancing the microscopic $\mathbb{Z}_n$ symmetry of discrete ferromagnets to a U(1) symmetry at the macroscopic scale. Proliferation of domain wall defects results in the formation of numerous domains and the spins are able to change their orientation by arbitrary amounts over large distances in a manner such that the macroscopic order parameter exhibits angular fluctuations uniformly along all directions [1]. In some ferromagnets, however, discrete vortices proliferate simultaneously with domain walls and disorder the system before the U(1) symmetry emerges. A forced suppression of vortices, in such cases, can delay their proliferation and allow the intermediate U(1) phase to manifest itself.

On the square lattice, $\mathbb{Z}_n$ ferromagnets with $n \geq 5$ exhibit an intermediate U(1) phase without vortex suppression [1–8, 28]. The direct order-disorder phase transition in the $\mathbb{Z}_3$ (three state Potts) ferromagnet, on the other hand, was recently shown to split under strong suppression of vortices and an intermediate U(1) phase was uncovered [9]. The $\mathbb{Z}_4$ Ashkin Teller ferromagnet also undergoes a direct order-disorder transition [10]. The interplay between vortices and domain walls at this transition is known to generate a line of continuously varying critical exponents [11]. A decoupling of this interplay and demonstration of an extended phase where a microscopic $\mathbb{Z}_4$ symmetry enhances to U(1) has interesting implications for quantum phase transitions in antiferromagnets [12–14], melting of crystal films [1] and adsorption of gas particles on metal surfaces [15–19]. Can the suppression of vortices open up a U(1) phase in this model as well?

In this article, we show that suppression of vortices in the $\mathbb{Z}_4$ ferromagnet on a square lattice indeed destroys the direct order-disorder transition and results in the formation of an intermediate phase with emergent U(1) symmetry. Interestingly, however, U(1) emergence is not the only possibility for the intermediate phase. Due the even parity of n in this model, we are able to distinguish between chiral vortices and non-chiral vortices. We show that a selective suppression of non-chiral vortices leaves the chiral vortices to proliferate in the intermediate phase. As a result, enhancement of the $\mathbb{Z}_4$ symmetry to a U(1) symmetry is replaced by restoration of chiral symmetry, i.e. a $\mathbb{Z}_2$ subgroup of the $\mathbb{Z}_4 \to \mathbb{Z}_2 \times \mathbb{Z}_2$ symmetry is restored. In order to verify that this phenomenon is not an artifact of the $\mathbb{Z}_4$ symmetry, we demonstrate U(1) emergence versus chiral symmetry restoration via vortex suppression in the $\mathbb{Z}_6$ ferromagnet as well. We conclude that this phenomenon can occur in all ferromagnets with even n.

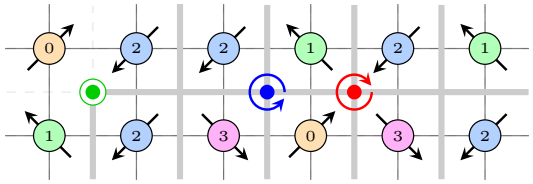

FIG. 1. (Color online) A $\mathbb{Z}_4$ spin configuration is shown with domain walls (gray), a non-chiral vortex (blue), a non-chiral antivortex (red) and a chiral vortex (green).

In a general $\mathbb{Z}_n$ ferromagnet, a spin s_i is placed at each vertex i of a lattice Λ (a square lattice in this case) and each spin can be in one of n different states $s_i \in \{0, 1, \ldots, n-1\}$ (Fig. 1). In the ordered phase a majority of the spins take up a common state while the states are taken up arbitrarily in the disordered phase. The vector order parameter which captures a direct transition between these two phases is defined for a system of L^2 spins as $m \equiv (m_x, m_y)$ where $m_x = L^{-2} \sum_i \cos 2\pi s_i/n$ and $m_y = L^{-2} \sum_i \sin 2\pi s_i/n$ [6, 8]. The macroscopic symmetry of the system is reflected in the distribution $P(m_x, m_y)$ of this order parameter.

Domain walls and vortex defects reside on the dual lattice Λ', which in this case is another square lattice shifted from Λ by half a lattice spacing along each direction [1, 3]. If two neighboring spins on Λ are in dissimilar states, then a domain wall is placed on the edge of Λ' separating the two spins (Fig. 1). Each vertex i' in Λ' is assigned a winding number

$$\omega_{i'} = (\Delta^n_{b,a} + \Delta^n_{c,b} + \Delta^n_{d,c} + \Delta^n_{a,d})/n \qquad (1)$$

which is essentially the finite difference equivalent of a circuit integral in continuum space when each elementary square plaquette in Λ is chosen as a circuit and the spins

at the four corners of each plaquette are in states a, b, c and d when traversed in an anticlockwise sequence. A vortex is present at i' if $\omega_{i'} = +1$ and an anti-vortex is present if $\omega_{i'} = -1$ (Fig. 1).

$\Delta_{a,b}$ represents the difference, modulo n, between states a and b. More precisely, this modular difference is calculated as

$$\Delta^n_{a,b} = \begin{cases} a-b-n, & \text{if } a-b > +n/2 \\ a-b+n, & \text{if } a-b \leq -n/2 \\ a-b, & \text{otherwise} \end{cases} \quad (2)$$

The asymmetry in this calculation is evident from the presence of an equality condition in $a - b \leq -n/2$. If a spin state s_i is viewed as two dimensional unit vector oriented at an angle $\theta_i = 2\pi s_i/n$, then this calculation restricts the angle difference to lie in $(-\pi, +\pi]$ [3, 26]. The asymmetry induced by the inclusion of $+\pi$ and exclusion of $-\pi$ is the origin of chirality in vortices. Consider, for example, a configuration of $\mathbb{Z}_4$ spins with states 0,1,2 and 2 arranged at the corners of a square plaquette when read in an anticlockwise sense (Fig. 1). The winding number for this plaquette, according to the above calculation is $+1$, indicating the presence of a vortex. If, on the other hand, we calculate the winding number by traversing the plaquette in a clockwise sense, then the winding number turns out to be zero, indicating the absence of vorticity. As we will show, this chirality that is built into the definition of vorticity can have fascinating consequences for the phase diagram of the system.

In order to highlight these consequences, we define a different type of vorticity which does not exhibit this chirality. A non-chiral version of the modular difference is formulated as

$$\Delta^{n,nc}_{a,b} = \begin{cases} a-b-n, & \text{if } a-b > +n/2 \\ a-b+n, & \text{if } a-b < -n/2 \\ a-b, & \text{otherwise} \end{cases} \quad (3)$$

The corresponding calculation for the winding number is

$$\omega^{nc}_{i'} = (\Delta^{n,nc}_{b,a} + \Delta^{n,nc}_{c,b} + \Delta^{n,nc}_{d,c} + \Delta^{n,nc}_{a,d})/n \quad (4)$$

The configuration of $\mathbb{Z}_4$ states 0,1,2 and 2, for example, results in zero vorticity with this definition when calculated either in clockwise or in anticlockwise sense. Vortex defects with $\omega^{nc}_{i'} \neq 0$ are termed as non-chiral vortices. The special defects which have $\omega^{nc}_{i'} = 0$ but $\omega_{i'} \neq 0$ are termed as chiral vortices.

The formation of vortices and antivortices can be suppressed by raising their core energy by an amount λ [9]. With the inclusion of such a term for suppressing standard vortices, the clock Hamiltonian for a $\mathbb{Z}_n$ ferromagnet becomes

$$\mathcal{H} = -\sum_{\langle i,j\rangle \in \Lambda} \cos 2\pi \left(s_i - s_j\right)/n + \lambda \sum_{i' \in \Lambda'} |\omega_{i'}| \quad (5)$$

Non-chiral vortices can be selectively suppressed by replacing the second term with $\lambda^{nc} \sum_{i' \in \Lambda'} |\omega^{nc}_{i'}|$.

We have simulated both these cases across a wide range of suppression strength and temperature T for different system sizes. In our simulation, spins were initialized to a completely ordered configuration and updated using the Metropolis single spin-flip algorithm as the plaquette based term for vortex suppression cannot be incorporated into cluster update algorithms [27]. The autocorrelation time for observables, which tend to be quite large for single spin-flip algorithms, was measured at each parameter point. Around 10^4 uncorrelated configurations were discarded for equilibriation following which measurements were made on 10^5 uncorrelated configurations.

For each configuration, we calculated the magnetization $|m| = \sqrt{m_x^2 + m_y^2}$, the angle of the order parameter $\phi = \arctan(m_y/m_x)$, the density of domain walls ρ_{dw} defined as the fraction of edges in Λ' containing a domain wall and the density for the different types of vortex defects, defined as the fraction of vertices in Λ' containing a defect of the given type. ρ_{vx} represents the density of standard vortices with $\omega_{i'} \neq 0$, ρ_{ncvx} represents the density of non-chiral vortices and ρ_{cvx} represents the density of chiral vortices.

In the pure $\mathbb{Z}_4$ clock ferromagnet ($\lambda = 0$), the magnetization decays to zero across the direct order-disorder phase transition at $T \sim 1.1$ (Fig. 2). The pattern of symmetry breaking in the low temperature phase is captured by $\langle \cos 4\phi \rangle$ which takes a value $+1$ when the $\mathbb{Z}_4$ symmetry is broken. Both domain walls and vortices are observed to proliferate simultaneously near this transition, as indicated by an increase in their densities. When the formation of vortices is suppressed ($\lambda = 2$), the transition splits into two as indicated by the appearance of a two step decay in the magnetization. The first decay is accompanied by the proliferation of domain walls while the second one corresponds to the disordering transition driven by the proliferation of vortices. This behavior is similar to the one obtained with vortex suppression in the $\mathbb{Z}_3$ ferromagnet [9]. Spin configurations in the intermediate phase (Fig. 3(a)) show a few bound pairs of vortices and fragmented domains typical of quasi long range order [9]. This intermediate phase can be extended further by pushing the disordering transition to higher temperatures via strong suppression of vortices ($\lambda = 100$). When the formation of vortices is completely forbidden, the disordering transition vanishes and the system is left with a single transition from the $\mathbb{Z}_4$ symmetry broken phase to the emergent U(1) phase(Fig. 2). This result is interesting because a thermodynamically stable emergence of U(1) symmetry, which is usually reported only at the disordering transition point, is shown to appear throughout an extended phase in this case. However, as we show next, U(1) emergence is not the only possibility for the intermediate phase.

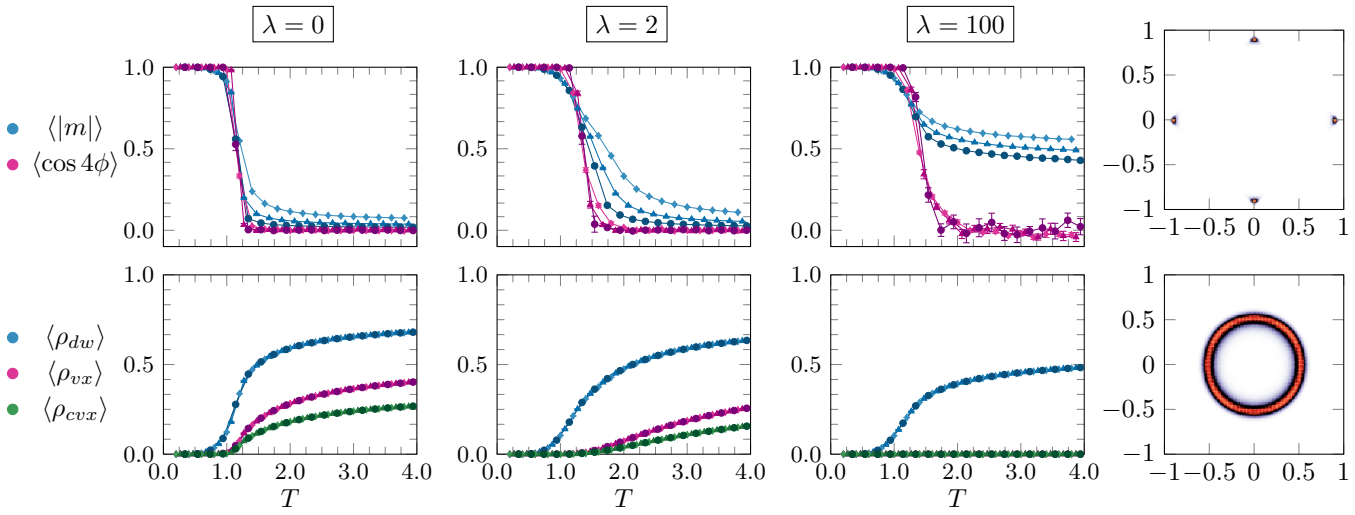

FIG. 2. (Color online) A split in the order-disorder transition and the appearance of an intermediate phase is shown to occur with increasing suppression strength λ. Observable values correspond to system sizes $L = 16$ (diamond), $L = 32$ (triangle) and $L = 64$ (circle). For $\lambda = 100$, vortices are nearly absent and only the domain walls are left to proliferate. The order parameter distribution $P(m_x, m_y)$ for a 32^2 system at this λ shows $\mathbb{Z}_4$ symmetry breaking in the ordered phase at $T = 1.1$ (top right) and enhancement to U(1) symmetry at $T = 3.0$ (bottom right).

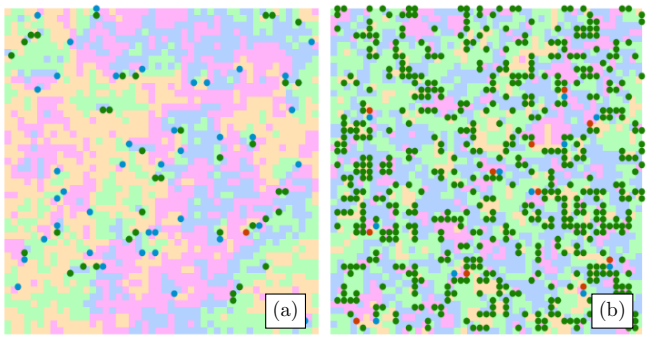

FIG. 3. (Color online) Typical spin configurations for a 48^2 system show (a) numerous domains and a few vortices in the emergent U(1) phase when standard vortices are suppressed, and (b) proliferation of chiral vortices in the chiral symmetry restored phase when non-chiral vortices are suppressed. Chiral vortices (green dots) are overlaid on the standard vortices (red and blue) in (a) and shown alongside non-chiral vortices in (b). Both configurations were generated at $T = 2.5$ with a suppression value of 4.

We return to the pure $\mathbb{Z}_4$ ferromagnet and begin a selective suppression of non-chiral vortices using a λ^{nc} term for (5). When $\lambda^{nc} = 0$, both chiral and non-chiral vortices proliferate simultaneously accompanied by the proliferation of domain walls across the direct order-disorder transition (Fig. 4). When the non-chiral vortices are suppressed ($\lambda^{nc} = 2$), the transition appears to split again. In this case, however, the proliferation of domain walls is closely followed by the proliferation of chiral vortices. With increasing λ^{nc}, the proliferation of both domain walls and chiral vortices remains unchanged while proliferation of non-chiral vortices is observed to weaken. The crucial difference in the pattern of symmetry breaking on the high temperature side is captured by $\langle \cos 4\phi \rangle$, which changes its sign to a negative value. This represents the restoration of $\mathbb{Z}_2$ chiral symmetry and indicates a transition from order to incomplete order [20]. Examples of similar $\mathbb{Z}_2$ symmetry restored phases are the $\langle \sigma \rangle$ phase of the Ashkin Teller model obtained beyond the clock point in three dimensions [21] and the disordered flat phase in restricted solid-on-solid models of crystal growth [22]. Typical spin configurations obtained for this phase clearly reveal the proliferation of chiral vortices (Fig. 3(b)). Interestingly, the full $\mathbb{Z}_n$ symmetry is never restored at any value of temperature above the chiral symmetry restoring transition. Instead, $\langle \cos 4\phi \rangle$ appears to become more negative with increasing L (Fig. 4), indicating the persistence of a thermodynamically stable chiral symmetry restored phase even at high temperatures. This result suggests that proliferation of non-chiral vortices is not strong enough to drive a disordering transition and accompanies a gradual crossover to disorder instead.

The restoration of a $\mathbb{Z}_2$ symmetry raises an important question: is this phenomenon a special feature restricted to the $\mathbb{Z}_4$ ferromagnet, possibly because it can be decomposed into a $\mathbb{Z}_2 \times \mathbb{Z}_2$ model? While defining the non-chiral vortices, we had not restricted ourselves to $n = 4$. The distinction between chiral and non-chiral vortices was made possible using the asymmetry of modular differences for the particular case when $\Delta_{a,b} = -n/2$ in (3). Such cases appear when n is even. It should, therefore, be possible to verify whether the replacement of U(1) emergence by chiral symmetry restoration occurs in models

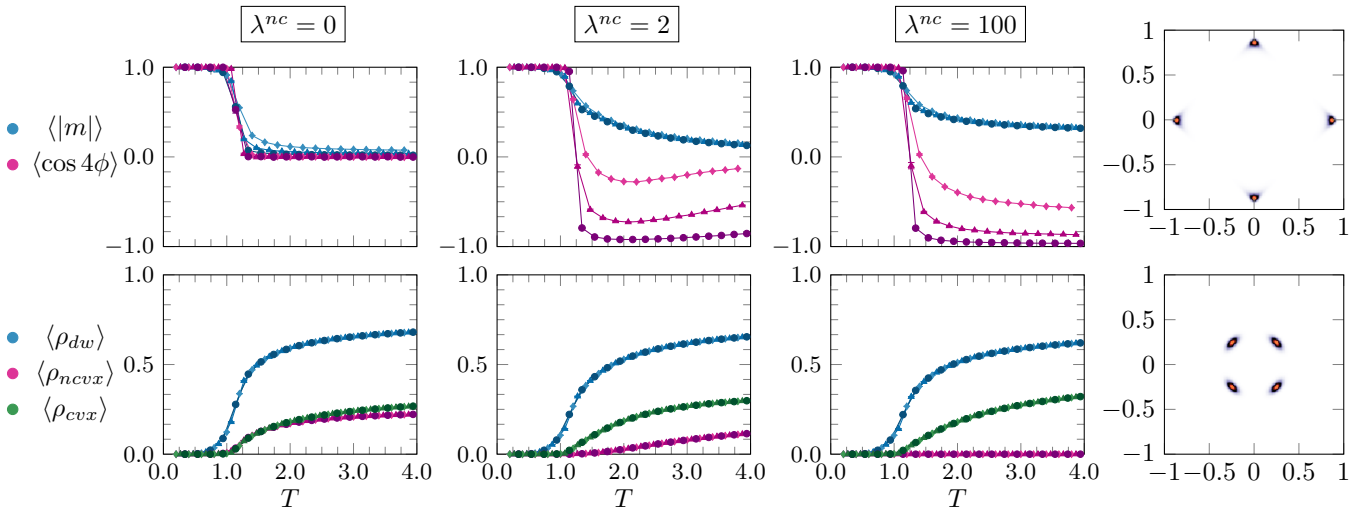

FIG. 4. (Color online) The order-disorder transition is replaced by a chiral symmetry restoring transition when non-chiral vortices are suppressed using increasing values of λ^{nc}. The $\mathbb{Z}_4$ symmetry breaking at $T = 1.1$ in the ordered phase (top right) and chiral symmetry restoration at $T = 3.0$ (bottom right) are clearly reflected in the order parameter distribution obtained for a 32^2 system with $\lambda^{nc} = 100$. System sizes used to calculate observable statistics are the same as those in Fig. 2.

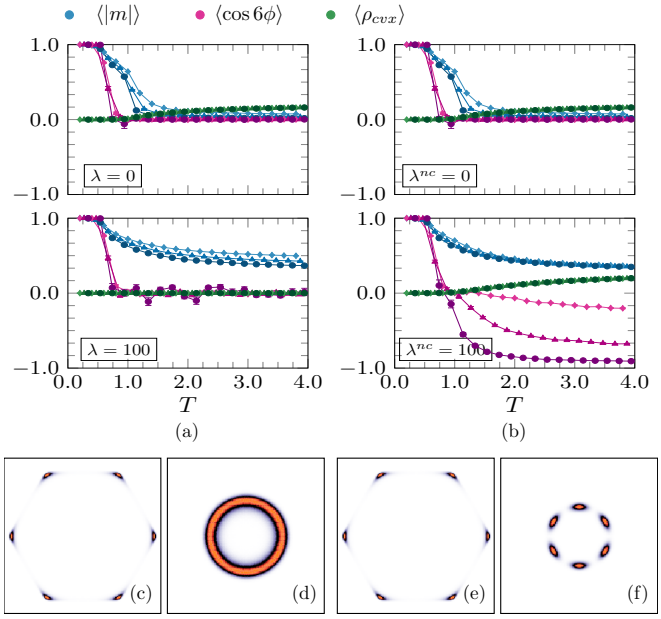

FIG. 5. (Color online) The emergent U(1) phase in the $\mathbb{Z}_6$ clock ferromagnet is (a) shown to extend upon suppression of standard vortices, and (b) shown to get replaced by a chiral symmetry restored phase upon suppression of non-chiral vortices. The order parameter distribution shows that the $\mathbb{Z}_6$ symmetry is broken in the ordered phase in both cases of suppression (c) and (e), but gets enhanced to U(1) in the former (d), and replaced by chiral symmetry restoration in the later (f).

with higher even values of n as well.

We have simulated the $\mathbb{Z}_6$ clock ferromagnet on the square lattice with different types of vortex suppression. This model exhibits a narrow intermediate U(1) phase even without the suppression of vortices [3, 5, 8]. When we suppress the formation of the standard vortices, the U(1) phase is observed to extend further upto higher temperatures and chiral vortices are nearly absent in the phase (Fig. 5). On suppression of non-chiral vortices, however, the chiral vortices are left behind to proliferate and they drive a phase transition from the ordered phase to a chiral symmetry restored phase. The symmetry restoration is clearly reflected in the order parameter distribution and in $\langle \cos 6\phi \rangle$ which changes sign across the transition. This result confirms that chiral symmetry restoration is realizable in general $\mathbb{Z}_n$ ferromagnets with even values of n.

The subtle difference between the proliferation of standard vortices, which contains both chiral and non-chiral defects, and the proliferation of chiral defects highlights the crucial role played by these topological defects in determining the phase diagram of $\mathbb{Z}_n$ ferromagnets. Our result can have interesting implications for phase transitions in a variety of other systems like superfluids and superconductors which are also governed by the proliferation of vortex defects [23, 24]. Moreover, our demonstration provides a simple example of how the symmetry information contained inside topological defects can determine the symmetry of the phase in which they proliferate. It would, therefore, be interesting to apply our technique and open up richer phase diagrams for systems like liquid crystals [25] in which the defects are associated with higher symmetries.

* sbhtta@imsc.res.in

[1] M. B. Einhorn, R. Savit, and E. Rabinovici, Nucl. Phys. B **170**, 16 (1980).
[2] J. V. José *et al.*, Phys. Rev. B **16**, 1217 (1977).
[3] G. Ortiz, E. Cobanera, and Z. Nussinov, Nucl. Phys. B **854**, 780 (2012).
[4] J. Fröhlich and T. Spencer, Commun. Math. Phys. **83**, 411 (1982).
[5] C. M. Lapilli, P. Pfeifer, and C. Wexler, Phys. Rev. Lett. **96**, 140603 (2006).
[6] S. K. Baek, P. Minnhagen, and B. J. Kim, Phys. Rev. E **80**, 060101 (2009).
[7] A. C. Van Enter, C. Külske, and A. A. Opoku, J. Phys. A **44**, 475002 (2011).
[8] O. Borisenko *et. al.*, Phys. Rev. E **85**, 021114 (2012).
[9] S. Bhattacharya and P. Ray, arXiv:1507.08766 (2015).
[10] R. J. Baxter, *Exactly Solved Models in Statistical Mechanics* (Courier Corporation, 2007).
[11] L. P. Kadanoff, Ann. Phys. (N.Y.) **120**, 39 (1979).
[12] A. W. Sandvik, Phys. Rev. Lett. **98**, 227202 (2007).
[13] R. G. Melko and R. K. Kaul, Phys. Rev. Lett. **100**, 017203 (2008).
[14] J. Lou, A. W. Sandvik, and L. Balents, Phys. Rev. Lett. **99**, 207203 (2007).
[15] K. Binder, W. Kinzel, and D. P. Landau, Surf. Sci. **117**, 232 (1982).
[16] H. C. M. Fernandez, J. J. Arenzon, and Y. Levin, J. Chem. Phys. **126**, 114508 (2007).
[17] M. E. Zhitomirsky and H. Tsunetsugu, Phys. Rev. B **75**, 224416 (2007).
[18] X. Feng, H. W. J. Blote, and B. Nienhuis, Phys. Rev. E **83**, 061153 (2011).
[19] K. Ramola, K. Damle, and D. Dhar Phys. Rev. Lett. **114**, 190601 (2015).
[20] N. Todoroki, Y. Ueno, and S. Miyashita Phys. Rev. B **66**, 214405 (2002).
[21] R. V. Ditzian, J. R. Banavar, G. S. Grest, and L. P. Kadanoff Phys. Rev. B **22**, 2542 (1980).
[22] Peter B. Weichman and Anoop Prasad Phys. Rev. Lett. **76**, 2322 (1996).
[23] G. Kohring, R. E. Shrock, and P. Wills, Phys. Rev. Lett. **57**, 1358 (1986).
[24] S. R. Shenoy, Phys. Rev. B **42**, 8595 (1990).
[25] P. E. Lammert, D. S. Rokhsar, and J. Toner, Phys. Rev. Lett. **70**, 1650 (1993).
[26] E. Bittner, A. Krinner, and W. Janke, Phys. Rev. B **72**, 094511 (2005).
[27] D. P. Landau and K. Binder, *A Guide to Monte Carlo Simulations in Statistical Physics* (Cambridge University Press, 2014).
[28] S. Elitzur, R. Pearson, and J. Shigemitsu, Phys. Rev. D **19**, 3698 (1979).